https://doi.org/10.32056/KOMAG2025.14

Checking the technical condition of an energy storage device made of lithium-iron-phosphate cells supervised by a passive BMS system

Received: 12.05.2025

Accepted: 02.10.2025

Published online: 09.10.2025

Piotr HYLLA[1], **Wojciech KURPIEL**[1*], **Taras DMYTRIV**[2]

Author's affiliations and addresses:

[1] KOMAG Institute of Mining Technology, 37 Pszczyńska Street

44-101 Gliwice, Poland

[2] Department of Aviation and Manufacturing Engineering and Transport, Lviv Politechnic National University,

79013 Lviv, Ukraine

*** Correspondence:**

e-mail: wkurpiel@komag.eu

Abstract:

Pandemics, wars, restrictions and restrictions can disrupt supply chains and make trade between countries and even continents difficult. This situation caused that energy storage devices which were not prepared for operation to be stored for several years. Even an unused energy storage device loses its capacity. The article presents and discusses the results of testing the 400 Ah energy storage device focusing on checking how the parameters such as voltage, current and temperature affect the capacity of cells after a long period of non-use. This type of tests can provide valuable information on the maintenance and optimal storage of energy storage devices.

Keywords: lithium battery, passive cell balancing, battery, energy storage

Publisher: **KOMAG Institute of Mining Technology, Poland**

1. Introduction

Dynamically changing situation in Europe and the world in the early 2020s caused by the effects of the COVID-19 pandemic and the ongoing armed conflicts in Europe and the Middle East forced acceleration of decarbonization process [1]. This necessity is mainly related to the fact that the suppliers of energy raw materials are the countries with an unstable political situation and often covered by international sanctions. Current policy of the European Union on decarbonization of industry and increasing the share of renewable energy sources is included in the EU act on carbon neutral industry (COM (2023) 161, SWD (2023) 68) published on 16 March 2023. These actions are aimed at increasing the development of zero or low-emission technologies, especially in the power sector [2]. Renewable energy sources are also becoming increasingly popular in Poland, which is particularly visible in the number of installed RES (Renewable Energy Sources), which, according to the Energy Market Agency, increased year-on-year by 20% from 24,900.7 MW in 2023 to 29,862.4 MW in 2024. The largest increase is in photovoltaic installations 30.5% and wind turbines 8.1% [3]. Hybrid installations have a significant increase of 21%. The most popular RES based on solar energy and wind speed are unstable sources with a periodic and unpredictable nature of operation [4]. Another disadvantage of these installations is the fact that the periods of production and demand are shifted relative to each other in time, which in most cases prevents the effective use of RES to power facilities without installing the additional energy storage device [5]. Currently, lithium batteries are one of the most commonly used energy storage devices [6]. The great popularity of lithium cells results from the advantages of this technology such as: high energy density, long life cycle, possibility of relatively fast charging, high efficiency and low self-discharge, which is the subject of the research work presented in this article [7]. Self-discharge is a process resulting from the internal resistance of the cell, causing the discharge of an unused battery, e.g. during transport or storage [8]. The events from the beginning of this decade resulted in the interruption of supply chains, lack of availability of components for manufacturing and limited demand, which also affected the lithium cells, which remained unused for months or even years.

This article presents and discusses the test results of a 400 Ah battery made of lithium-iron-phosphate ($LiFePO_4$) cells, which was brand new and stored at KOMAG for approximately two years without use. The tests consisted in measuring the voltage drop, current and temperature and calculating the capacity of the battery cells.

2. Materials and Methods

2.1. Energy storage

The battery is made of lithium iron phosphate ($LiFePO_4$) cells with a nominal voltage of 3.2 V and a capacity of 100 Ah (Figure 1). The cells are connected in a series-parallel arrangement. The battery consists of 212 series-connected packs giving 678.4 V DC nominal voltage, while each pack is a parallel connection of four cells, which gives a capacity of up to 400 Ah. The whole consists of 848 cells. Lithium-iron-phosphate ($LiFePO_4$) technology combines the advantages of high current efficiency, high energy density, safety and long service life. $LiFePO_4$ cells are particularly suitable for high-current applications. They can be discharged with a continuous current of up to 0.3C and charged with a current of up to 0.3C. They have a nominal voltage of 3.2 V and can operate in the voltage range from 2.5 V to 3.65 V. The designed service life of the cells reaches several thousand charge/discharge cycles. The cells show increased resistance to improper operating conditions compared to other lithium-ion technologies. However, in accordance with the applicable legal regulations regarding the manufacture of power supply systems based on lithium batteries, they require the use of an appropriate protection system.

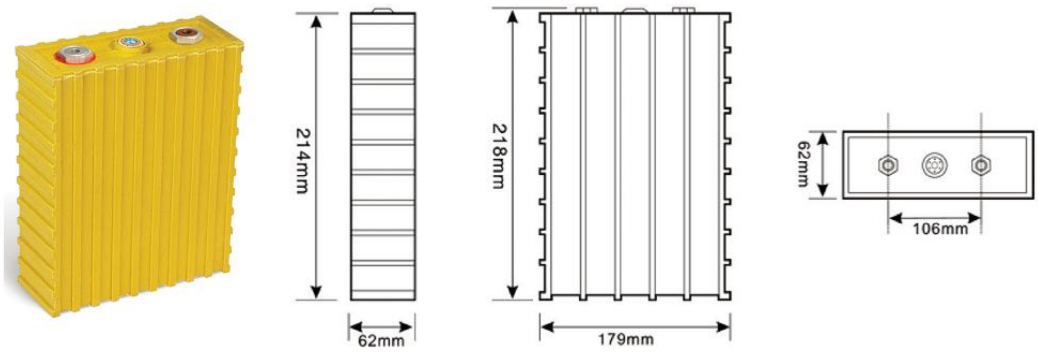

Fig. 1. Winston LFP100AHA WIDE cell [[9]]

Table 1. Technical data of Winston LFP100AHA cell [9]

Parameter	Value
Cell type	Winston LFP100AHA WIDE cell
Rated voltage	3.2 V DC
Maximum voltage	3.65 V DC
Minimal voltage	2.50 V DC
Capacity	100 Ah
Operating temperature	-45°C ÷ + 80°C
Mass	3.6 kg

The battery (Figure 2) is protected by two passive BMS ORION systems. The first one acts as a master and the second one as a slave. BMS (Battery Management System) systems prevent damage to lithium cells. They have a number of functions, such as: measurement of the system voltage, current and temperature, cell charge level, current and voltage protection of cells, temperature management, control of the charging/discharging procedure, data acquisition, communication with internal and external modules, monitoring and storing the previous data. The most important task of these systems is to equalize the voltage on the battery cells, called the cell balancing. The passive balancing current of the BMS system from the ORION family is up to 200 mA. Detailed information on the BMS system parameters is presented in [10], and the technical parameters of the battery are presented in Table 2.

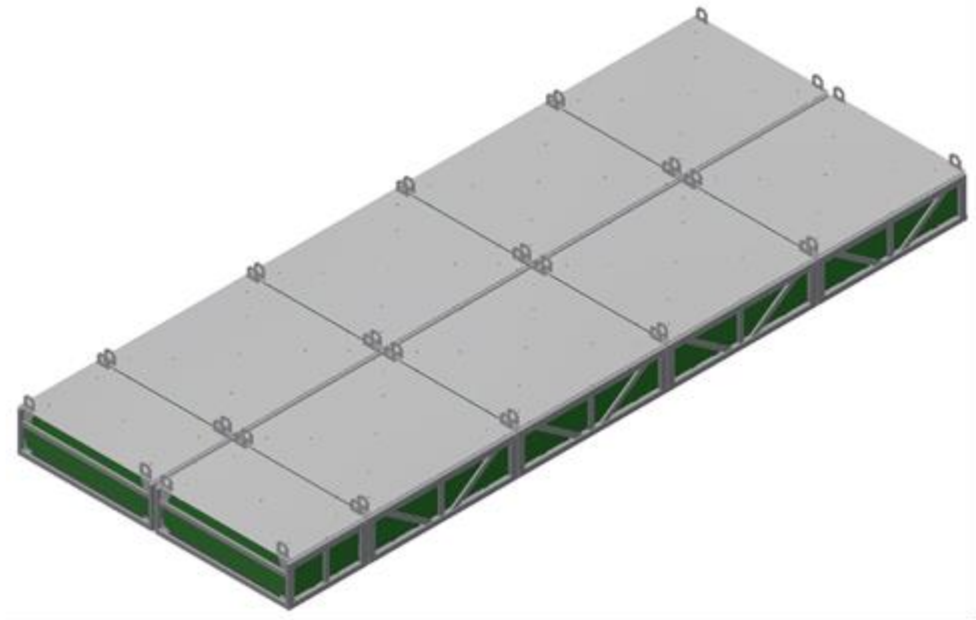

Fig. 2. Energy storage - illustrative drawing

Table 2. Battery technical parameters

Parameter	Value
Nominal voltage	678.4 V DC
Maximum voltage	773.8 V DC
Minimum voltage	530.0 V DC
Capacity	400 Ah
Number of cells	848 pieces
Energy	300 kWh
Maximum current	1200 A (15 minutes maximum)
Operating temperature	-45°C ÷ + 80°C
Configuration	212S4P
Geometric dimensions	5425 x 2380 x 365 mm
Weight	4500 kg

Difference in the amount of energy stored in each cell connected in series in a battery system has a very significant impact on the battery life. Without a BMS system, the voltage in each cell can differ significantly over time. Capacity of the battery pack can also quickly decrease during its operation, which results in the loss of usability of the battery system for further operation.

Publisher: **KOMAG Institute of Mining Technology, Poland**

2.2. Measuring station

Battery tests involving discharging and charging cells with different currents used a bidirectional programmable DC power supply. A four-pole GE0800DT4 type isolating switch was used to connect and disconnect the battery from the programmable power supply in a currentless state. Additionally, HX460 GIGAVAC type contactors were used to connect and disconnect the battery and the programmable power supply, as well as a fuse with a rated current of 350 A. The IT6108C-1500-240 bidirectional programmable DC power supply acts as a battery load and a battery charger in the test system. It integrates the source and sinks functions in one device. Based on these two functions, it offers the functionality of a two-quadrant operation. Ability to regenerate allows to recover the used energy back to the network, saving energy and cooling costs, without disturbing the network.

The bidirectional programmable power supply provides a maximum output voltage of up to 1500 V, support for a master-slave connection in parallel with averaging the current distribution, and a maximum output power of up to 108 kW.

The test station was assembled according to the electrical schematics (Figures 3 and 4). Figure 3 shows the connection diagram of the main switch, power fuse, contactor, and programmable power supply, which serves as the main energy receiver. This schematic illustrates a test setup with a single power supply, intended for testing the battery at a maximum discharge current of 160 A, a charge current of 140 A, and a charging voltage of 770 V.

Figure 4 presents the schematic of the test setup with two programmable power supplies, enabling battery discharge at currents above 160 A but not exceeding 310 A, and charging at 270 A with a voltage of 770 V.

The charging voltages of the cells were in accordance with the values specified in the manufacturer's technical documentation.

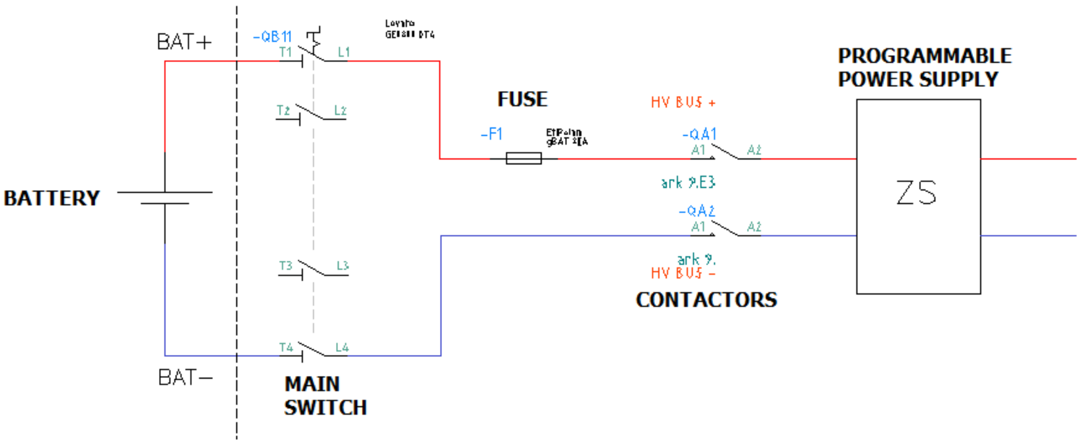

Fig. 3. Electrical diagram of the test system with one power supply unit - main power circuits

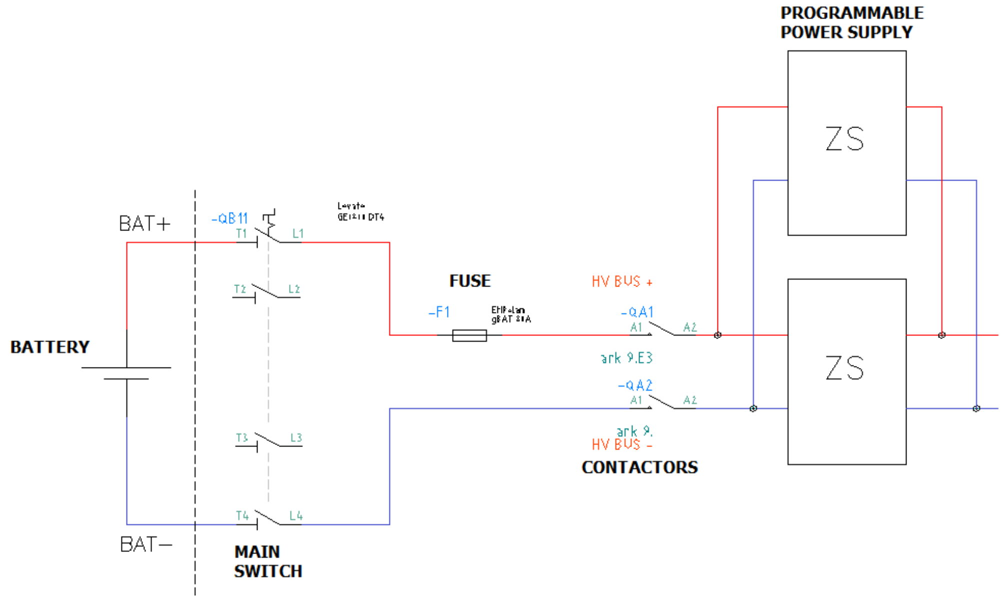

Fig. 4. Electrical diagram of the testing system with two power supply units - main power circuits

2.3. Software

The orionbms2_utility_stable.exe. program is used to configure the BMS ORION system of the device. The range of saved frames are adjusted to the addresses used by the BMS system. Due to the size of the resulting files, in a longer recording period, it was decided to save data with a resolution of approx. 500 ms. The information is saved in a CSV file. Direct displaying the contents of the saved files is possible on the computer screen (Figure 5) in real time.

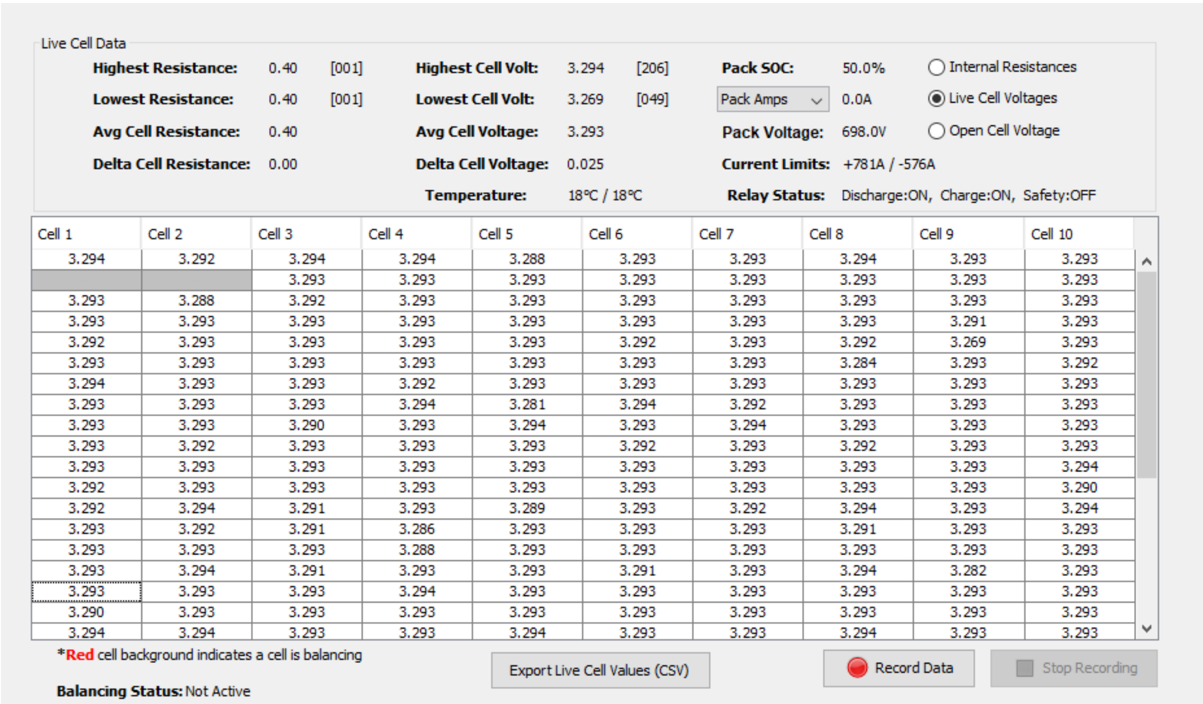

Fig. 5. Display of the configuration parameters of the BMS ORION system

Text files can be processed, for example, in a spreadsheet (e.g. MS Excel) or using scripts in Matlab / Octave / Python environments, etc. File processing allows for displaying and visualizing data. Therefore, it was decided that as part of the work, the collected data will be converted to text (CSV files) and then processed using an original script in the Matlab environment for visualization and analysis.

The analysis can be supported by the "asammdf GUI" program for quick visualization of file content. In this program, after importing the CAN signal database (exported from the BMS ORION system), it is possible to draw already scaled signals (e.g. voltage in volts, logical signals 0/1), however, there are difficulties in interpreting negative numbers (charge / discharge current). For this reason, this tool will be used only for data preview, before the final analysis in the Matlab package.

3. Results

The tested battery was brand new and had not been previously used in any other applications. Before the main tests began, it underwent a formation procedure consisting of several (fewer than ten full) charge and discharge cycles, aimed at stabilizing its operating parameters. The voltage at the battery terminals before the first test was 697 V.

The test focused on monitoring the technical condition of a 400 Ah battery, made of 848 lithium-iron-phosphate ($LiFePO_4$) cells. During the test, the basic parameters of the battery were recorded, analyzing the battery technical condition through multiple charge and discharge cycles using the power supply unit programmed to the limit values specified by the manufacturer.

During each cycle, the battery capacity was tested, making calculations after each charge and discharge process. Comparative tests included various values of discharge and charge currents, which allowed for an analysis of the impact of these parameters on the battery capacity. The results obtained during the tests were compared with the capacity declared by the manufacturer to assess the compliance of the actual and theoretical parameters.

The average battery capacity was determined based on the results obtained from 14 discharge and charge cycles, which allowed for obtaining reliable and representative data on its performance.

The subsections present sample waveforms illustrating the recorded data. In the case of tests 1 and 2, three discharge and charge cycles were performed, in the case of tests 3 and 4 – two cycles, while in the remaining cases – one test cycle. The graphs were obtained using the original script developed in the Matlab environment. The SOC (State of Charge) value used in the analysis was retrieved by computer software from the BMS system.

3.1. Test 1 discharge current 120 A

The subsection presents examples of voltage, current and temperature curves during battery discharge with a current of 120 A. Figure 6a shows the characteristics of the battery cell voltages. Information about the voltage in the cell with the lowest ("min") and highest ("max") voltage is sent by the battery management system (BMS) via the CAN (Controller Area Network) bus. For comparison, the average voltage ("avg") of the cell was also added, calculated based on the battery voltage read from information sent by the BMS and the number of cells connected in series (212 in this case).

The next graph (Figure 7) is related to the temperature curves during the test. The BMS sends the highest and lowest temperature values ("max" and "min" in Figure 7). The presented cases show that the maximum temperature on the cells in the battery reached 30°C and did not exceed the maximum cell operating temperature permitted by the manufacturer. The discharge process began with charging the battery with a current of 120 A to the maximum voltage (approx. 3.65 V) on a single cell i.e. 773,8 V of the battery, what took about 50 minutes. Then, for the next 43 minutes, the energy storage unit remained unloaded, during which the maximum voltage dropped and stabilized to a level of approx. 3.35 V on a single cell with a total battery voltage of 709.1 V. Discharge process with a current of approx. 120 A took 3 hours 50 minutes until the voltage on the weakest single cell was below 2.5 V. At the end of discharge, total voltage on the battery was 661.2 V, and the SOC was 3.5%. The voltage on the strongest cell, i.e. the one with the most stored energy after discharge, was 3.13 V. The lowest temperature after the end of discharge recorded on the cells was 25°C, while the highest was about 29°C.

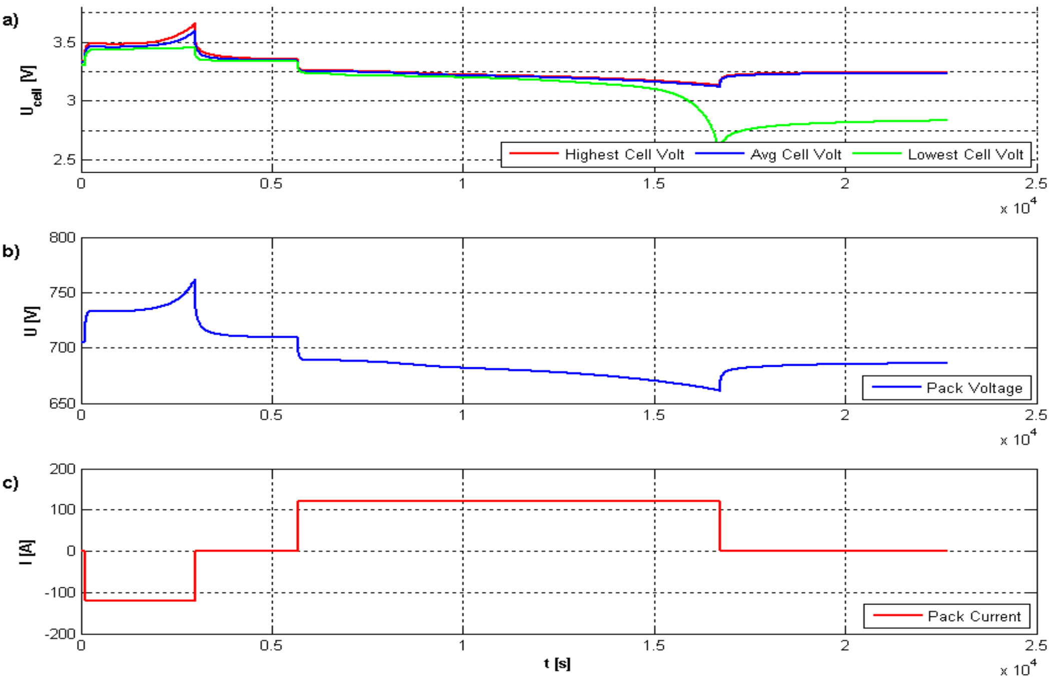

Fig. 6. Examples of results recorded by the BMS system during battery discharge: a) cells with the highest and lowest voltage in the battery, b) battery voltage, c) battery current

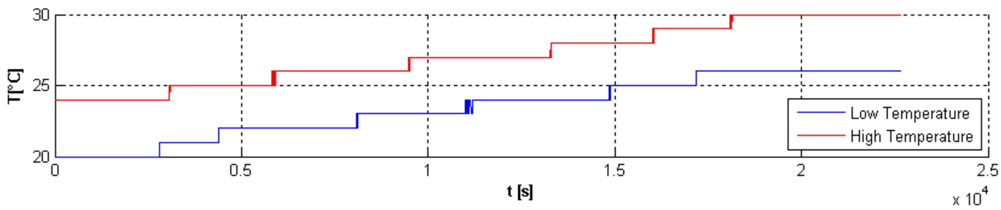

Fig. 7. Examples of results recorded by the BMS system during battery discharge: the highest and lowest temperature recorded on the sensors installed in the battery

The next graph (Figure 8) contains the characteristics of the voltages of the weakest cells in the battery. Each of the cells in the battery was assigned a number (ID identifier) at the assembly and configuration stage. Information about the voltage on the cells together with their ID number is sent by the BMS system via the CAN bus. The cells with the lowest measured voltage were defined as the weakest cell. Cell with ID number 49 differs significantly from the other weakest cells. The lowest measured voltage on cell ID49 was below 2.5 V, while the voltage on other cells was in the range of 3.0-3.1V, where the average voltage on all cells was 3.189.

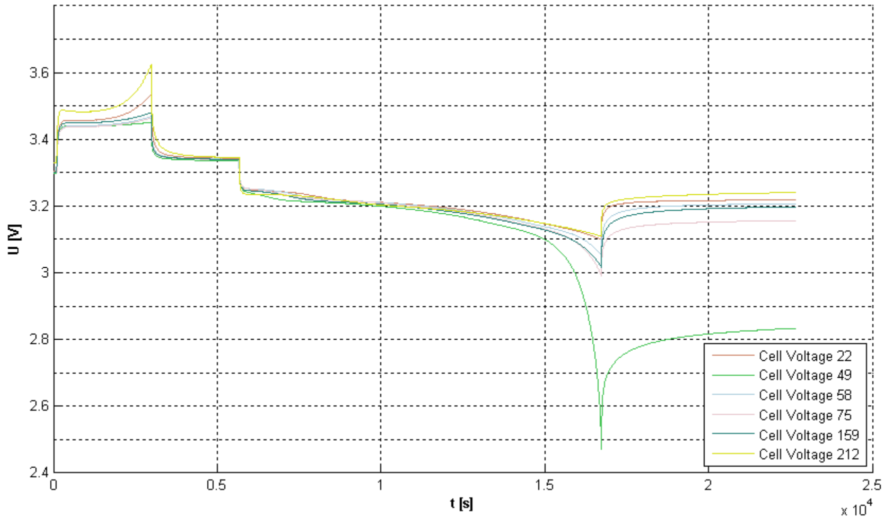

Fig. 8. Examples of the results recorded by the BMS system during battery discharge: cells with the lowest voltage

3.2. Test 1 charging current 120 A

The subsection presents sample voltage, current and temperature curves during battery charging with a current of 120 A. Figure 9 presents the voltage characteristics of the battery cells.

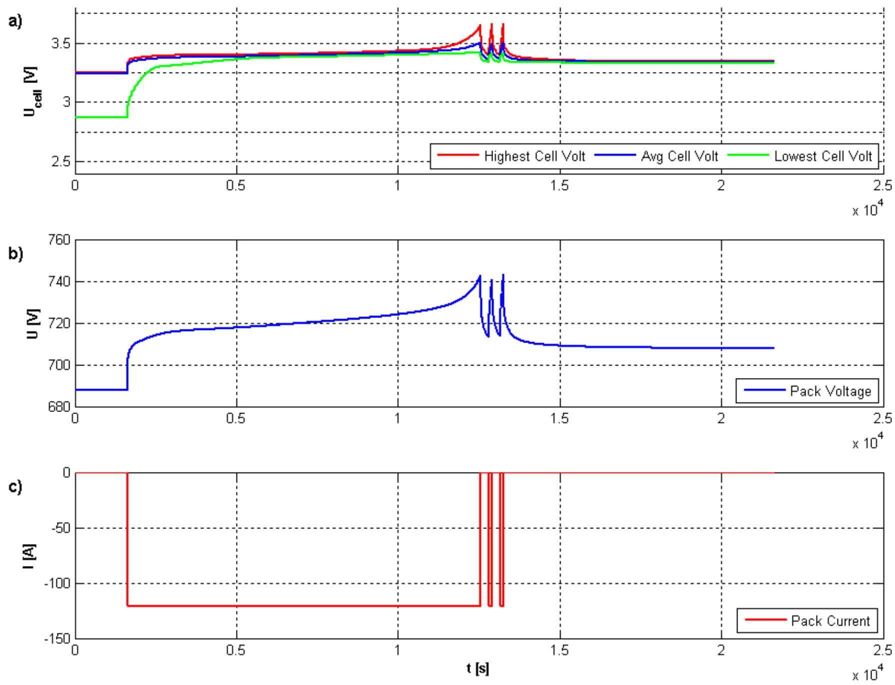

Fig. 9. Examples of the results recorded by the BMS system during battery charging: a) cells with the highest and lowest voltage in the battery, b) battery voltage, c) battery current

The graph shows that the charging process was preceded by 27 minutes of preparation in which the current was equal to 0. Then, charging was started with a constant current of 120 A for 3 hours 2 minutes from the SOC level of 3.5% to 95%, achieving a maximum voltage of 3.65 V on the strongest cell, an average cell voltage of 3.5 V and 3.4 V on the weakest cell. At the end of the first charging stage, the maximum voltage on the battery was 742 V. Then, for 11 minutes, the system tried to equalize the potential on each cell via the passive BMS system. The charging process was completed when the SOC indicator was 97.5%.

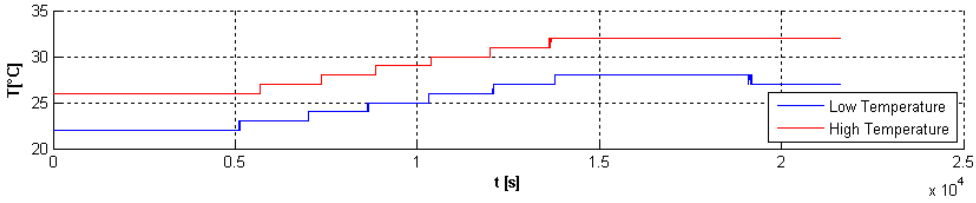

Fig. 10. Examples of the results recorded by the BMS system during battery charging: the highest and lowest temperatures recorded on the sensors installed in the battery

The graph (Figure 10) is related to the temperature curves. The presented cases show that the maximum temperature on the cells in the battery reached 32°C and did not exceed the maximum operating temperature of the cell permitted by the manufacturer. The temperature at the coldest point of the battery pack was 28°C. Maximum temperature at the beginning of the test was 26°C, and the lowest was 22°C. This means that the difference in both cases was 4°C, and none of the cells in the battery pack emitted excessive heat.

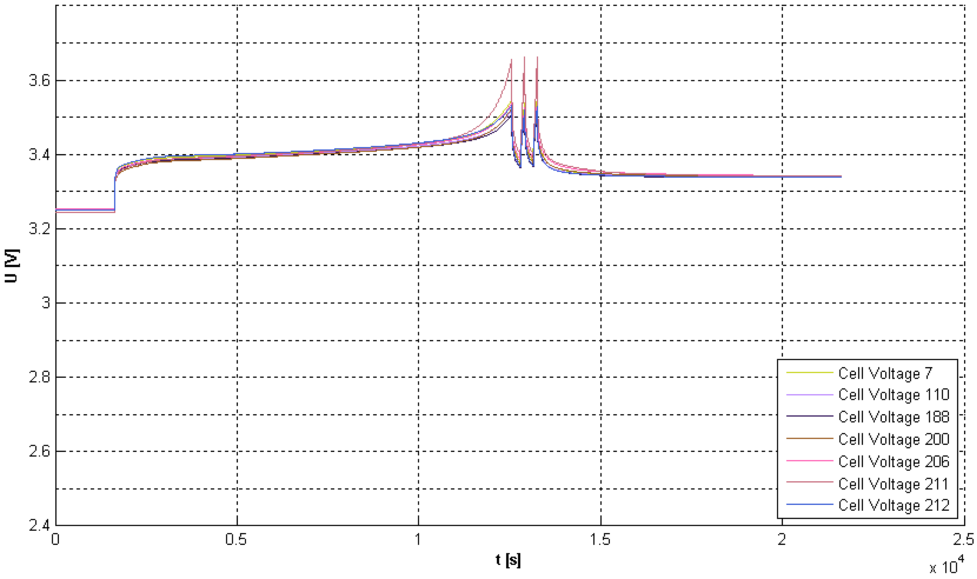

Fig. 11. Examples of results recorded by the BMS system while charging the battery: cells with the highest voltage

The next graph (Figure 11) shows the voltage characteristics of the strongest cells in the battery, along with the numbers (ID identifiers). Charging ended when the strongest cell (ID 211) reached a voltage of 3.65 V, while the voltage of the remaining 6 strongest cells was about 3.5 V, which corresponds to the average voltage on all cells.

Publisher: **KOMAG Institute of Mining Technology, Poland**

3.3. Test 4 discharge current 300 A

The next subsection presents examples of voltage, current and temperature curves during the battery discharge with a current of 300 A. This test was described as the presented current was the highest during the test. The discharge process lasted 1 h 13 min and ended when the weakest cell voltage was below 2.5 V (2.45 V) and the SOC parameter was 10%. From the graph in Figure 12a it can be concluded that the voltage changes on cell no. 212 (which is the weakest cell in the pack) differ significantly from the other cells. At the end of discharge, the difference between the strongest (3.09 V) and the weakest cell was 0.64 V, while the difference between the strongest and the average voltage of all cells (3.07 V) was only 0.02 V. The voltage of the battery after disconnecting the load was 651 V, then after some time stabilizing to the level of 687 V. At the moment of the measurement's completion voltage on the weakest cell was 2.82 V, and on the strongest 3.25 V, i.e. the difference was 0.43 V.

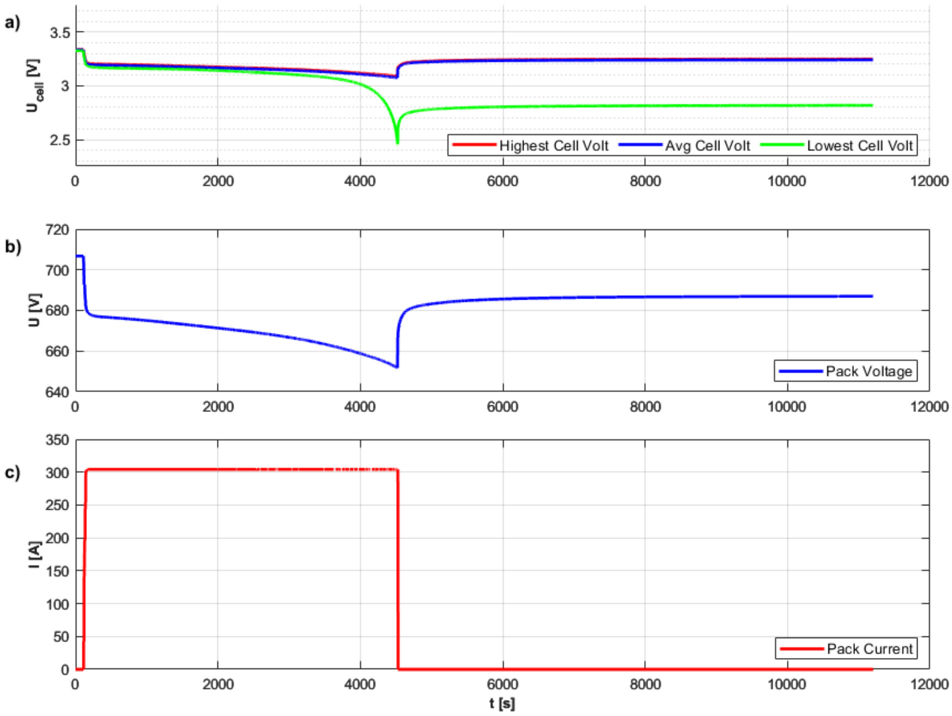

Fig. 12. Examples of the results recorded by the BMS system during battery discharge: a) cells with the highest and lowest voltage in the battery, b) battery voltage, c) battery current

Figure 13 shows temperature changes recorded by the BMS system during battery discharge. Before the discharge process began, the lowest temperature measured in the battery was 25°C, while the highest was 29°C. After the discharge was completed, temperature increased to a maximum 36°C and a minimum 31°C. From the presented data, it can be concluded that the battery warms up evenly, and the maximum measured temperature during discharge with a continuous current of 300 A does not exceed the permissible values given by the manufacturer.

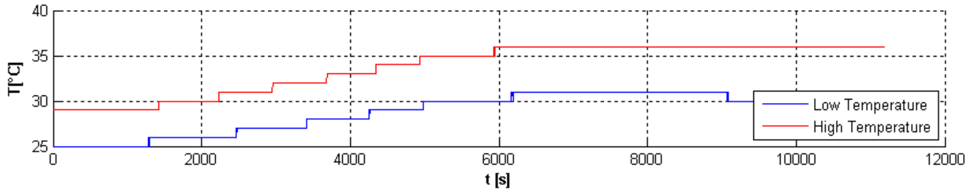

Fig. 13. Examples of results recorded by the BMS system during battery discharge: the highest and lowest temperature recorded by the sensors installed in the battery

The graph (Figure 14) contains the characteristics of the voltages of the weakest cells in the battery, along with their numbers (ID identifiers). Information about these cells is sent by the BMS system via the CAN bus. The graph shows a clear difference between the weakest cell ID 212 and the three other weakest cells. Differences in voltage changes indicated that the cell was not working properly, which may be due to a manufacturing defect or damage. Presence of a cell with such a defect significantly affects the operation of the entire battery, because it limits the functional capacity of the entire battery. This can be evidenced by the fact that the battery finished discharging when the SOC was 10%.

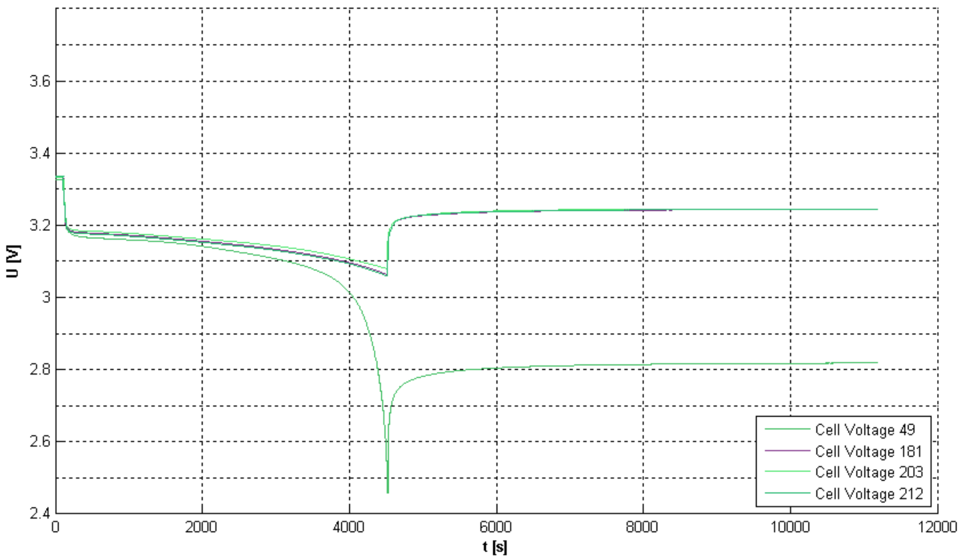

Fig. 14. Examples of the results recorded by the BMS system during battery discharge: cells with the lowest voltage

3.4. Test 4 charging current 270 A

This subsection presents the voltage, current and temperature curves during charging with the highest charging current of 270 A. The test began when the SOC indicator was 10% and the total voltage of the battery was 687.4 V. The first charging stage lasted about 1 h 20 min and ended when the strongest cell reached a voltage of 3.66 V and the voltage of the entire battery was 751.1 V. The average voltage on a single cell was 3.54 V and on the weakest cell was 3.46 V. At the end of the first charging stage, the SOC indicator was 53.5%. Balancing was the next charging stage, which consisted in equalizing the voltage on each cell and lasted about 3 min 20 s. Then the charging process was completed when the battery reached a charge level of 95% and the maximum voltage on the battery was 751 V. The maximum voltage on the strongest cell was 3.71 V, the lowest voltage on the weakest cell was 3.46 V, and the average voltage on single cells was 3.54 V. The presented data show (Figure 15) that the balancing process did not bring any significant effects. The reason for this is mainly the passive BMS system used with a balancing current of only 200 mA. To completely balance the battery, it is necessary to leave the battery in charging mode for many hours. Another solution that allows for faster battery balancing is to replace the balancer or the BMS with the components of a higher balancing current, e.g. 2 A. In the case of energy storage devices similar to the tested object, use of an active BMS system should be considered.

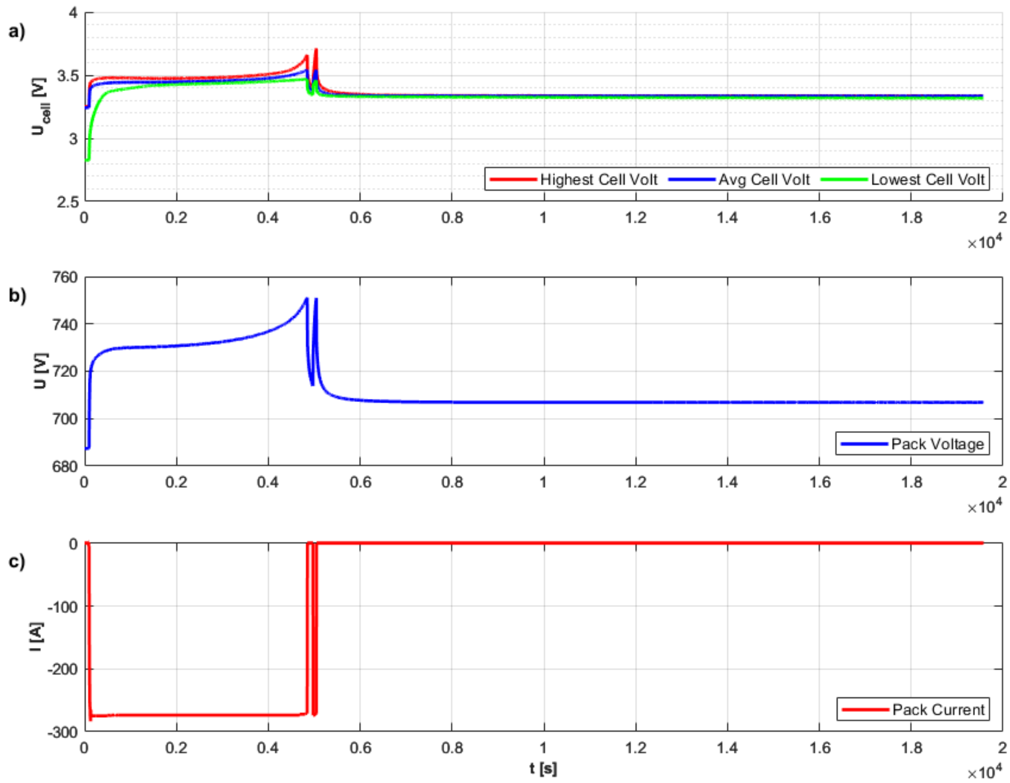

Fig. 15. Examples of the results recorded by the BMS system while charging the battery: a) cells with the highest and lowest voltage in the battery, b) battery voltage, c) battery current

The next graph (Figure 16) shows the temperature changes during the charging process, temperatures come from the sensors inside the pack of cells. The presented data show that the highest temperature measured before charging was 26°C, and the lowest 20°C. During the charging process, the temperature increased to a maximum 35°C, and minimum measured temperature at this point was 29°C.

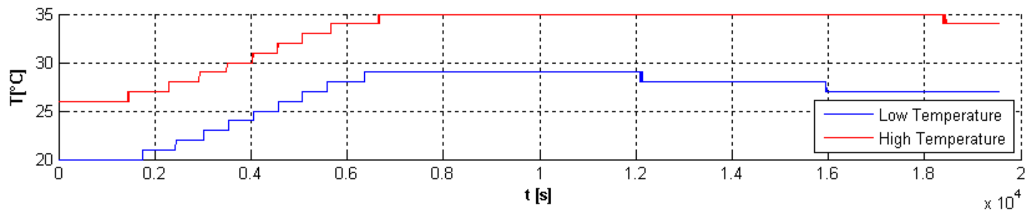

Fig. 16. Examples of the results recorded by the BMS system during battery charging: the highest and lowest temperatures recorded on the sensors installed in the battery

Publisher: **KOMAG Institute of Mining Technology, Poland**

The battery heats up slightly and evenly during charging, and there was no incident in which one of the cells emitted excessive heat. The maximum temperature measured during the test does not exceed the values that the cell manufacturer will include in the catalogue card. This means that there is no risk of damaging the battery when charging with a current of 270 A. After the charging process is complete, the battery cools down naturally.

The next graph (Figure 17) contains the voltage characteristics of the strongest cells in the battery, along with the numbers (ID identifiers). The highest voltage was recorded on cell no. 63, which differed from the average voltage on the cells by 0.12 V, while the difference between the 2 strongest cells was 0.06 V. The remaining strongest voltage levels are close to the average value. The balancing process should therefore mainly concern the cells no. 63 and 112.

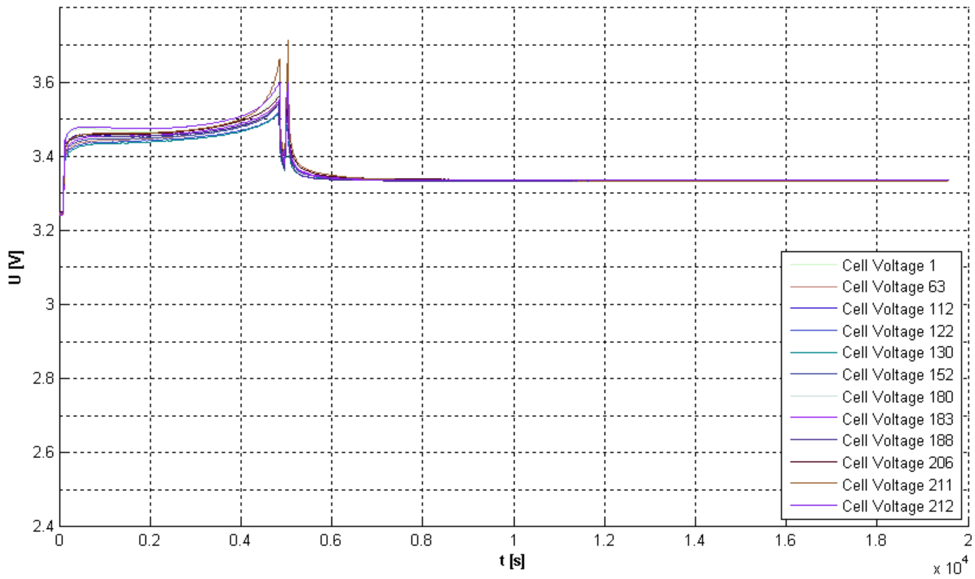

Fig. 17. Examples of the results recorded by the BMS system while charging the battery: cells with the highest voltage

4. Discussion

The objective of this research was to assess the technical condition of an unused battery with a nominal voltage of 678.4 V and a nominal capacity of 400 Ah. To achieve this, a series of charge and discharge cycles were conducted to evaluate the battery's current and voltage efficiency. The results obtained from these tests allowed for an assessment of the actual battery capacity compared to its nominal value.

During the tests, variations in charging currents relative to the discharge currents were observed. These discrepancies were primarily due to the power limitations of the programmable power supply units, which had a maximum power rating of 108 kW. For instance, in test 4, the intended charging current was 160 A, but due to these constraints, only 140 A was achieved. Additionally, a malfunction in one of the power supply units caused an interruption in testing. After the unit was repaired, it no longer achieved the expected power output of 108 kW, which impacted the charging current in test 8, where it was limited to 270 A instead of matching the discharge current of 300 A.

To determine the actual battery capacity, the charging and discharging times were recorded and analyzed. Battery capacity is defined as the product of current and time, representing the maximum amount of electric charge the battery can deliver over a specified duration. Since both charging and discharging occurred at constant current values, the capacity was calculated using the fundamental relationship (1, 2) [12]:

$$C = \int_0^t I(t)dt \quad (1)$$

$$C = I \cdot t \quad (2)$$

Were

C – battery capacity [Ah],

I – current [A],

t – time [h].

Uneven voltage distribution among the battery cells can significantly affect the total usable capacity. In the situation shown in the figure, a large difference between the minimum and maximum cell voltage can be seen, while the average voltage is close to the maximum value. This indicates that most cells are in good condition, and only a few cells have lower voltages.

Since the current flows through all cells in series, the cells with the lowest voltage and capacity limit the actual capacity of the entire pack. This means that even if the average voltage is high, the pack cannot deliver the full capacity corresponding to the average voltage – performance depends on the weakest cells.

Table 3 presents the calculated values for 14 tests covering charging and discharging processes and current and time parameters of each test.

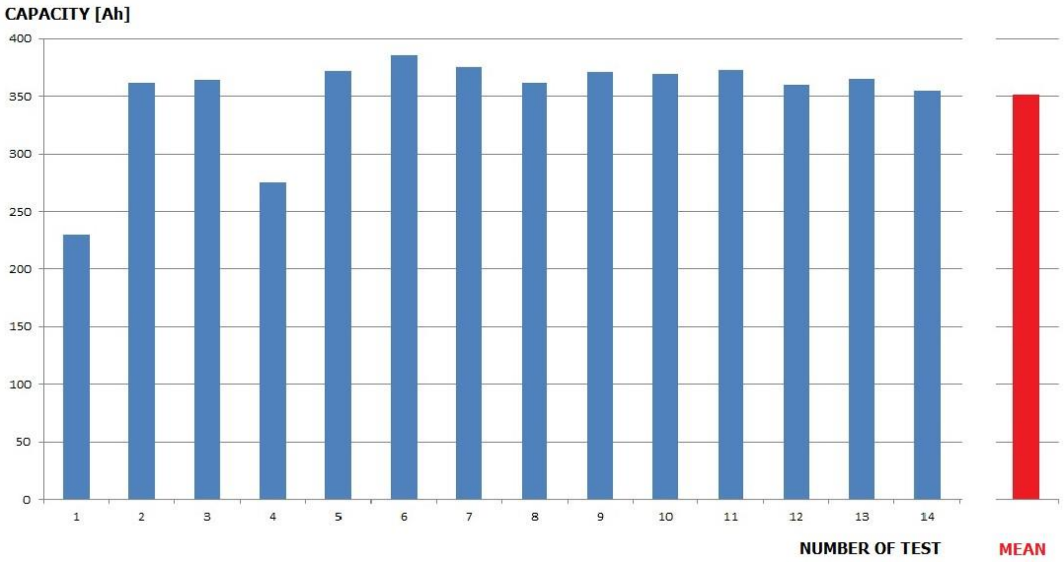

Fig. 18. Summary of the battery capacity

5. Analysis of Results

Table 3. Parameters with the calculated capacity

No. test	Cycle current	Current [A]	Time [h:min]	Capacity [Ah]
1	Discharging	120	1:54	230
	Charging	120	2:59	362
	Discharging	120	3:00	364
	Charging	120	2:16	275
	Discharging	120	3:04	372
	Charging	120	3:13	386
2	Discharging	160	2:19	375
	Charging	140	2:34	362
	Discharging	160	2:18	371
	Charging	140	2:36	369
3	Discharging	200	1:51	373
	Charging	200	1:47	360
4	Discharging	300	1:13	365
	Charging	270	1:19	355
Average capacity value				~351

Table 3 presents the recorded data and the calculated capacities for 4 test cycles. The results indicate that the battery's capacity consistently exceeded 350 Ah in most tests, with two exceptions: test 1 (230 Ah) and test 4 (275 Ah). These deviations may be attributed to experimental errors, inconsistencies in the power supply performance, or an uneven state of charge among the battery cells.

The overall average battery capacity across all tests was found to be 351 Ah, representing a 12.5% decrease from the nominal 400 Ah capacity. However, when excluding the two lowest capacity values (tests 1 and 4) as potential outliers, the recalculated average capacity was 367.8 Ah, indicating a more moderate degradation of 8.05%.

This reduction in capacity suggests that, despite being unused, the battery has experienced some level of degradation. Potential contributing factors to this decline include self-discharge, aging, and cell imbalance.

Batteries undergo self-discharge and aging even when not actively used. The chemical degradation of battery materials leads to a gradual decrease in capacity. Therefore, it is important to store batteries under proper conditions to minimize these effects. If batteries are not used for an extended period, they should be kept in a cool, dry place and regularly checked for their condition.

On the other hand, cell imbalance results from variations in the performance of individual cells. This can cause some cells to lose charge more quickly or reach full charge before others, leading to an uneven distribution of charge.

6. Conclusion

The battery's tested capacity remains relatively high, despite a measurable loss compared to its nominal rating. While the average loss of capacity (including all test results) is 12.5%, a refined analysis excluding potential outliers suggests a lower degradation of 8.05% (Figure 18). These findings indicate that the battery retains a significant portion of its original capacity and could still be effectively utilized in energy storage applications, though continued monitoring and further diagnostic tests may be necessary to fully assess its long-term performance.

References

[1] Hylla P., Mężyk A., Trawiński T., Polnik B.: Parameter estimation of PV system towards self-consumption of electric energy for dormitory. 11. Eur. Conf. Ren. Energy Sys. 18-20 May 2023, Riga – Latvia.

[2] Węgrzyn A., Spirydowicz A., Grebski W.: Dilemmas of the energy transformation in Poland 2021/2022. Min. Mach. 2022, 40, 32–42. https://doi.org/10.32056/KOMAG2022.1.4.

[3] Ministerstwo Klimatu i Środowiska, Agencja Rynku Energii S.A. (2024). Informacja statystyczna o energii elektrycznej. Biuletyn Miesięczny, Nr 5 (365), Maj 2024. Warszawa: Agencja Rynku Energii S.A. ISSN 1232-5457. Dostępne na: gov.pl/web/klimat oraz are.waw.pl. Author 1, A.; Author 2, B. Book Title, 3rd ed.; Publisher: Publisher Location, Country, 2008; pp. 154–196.

[4] Hylla P., Figiel A., Deja P., Skóra M.: Hybrydowe obiektowe magazyny energii, Materiały pokonferencyjne KOMEKO 2021, DOI: 10.32056/KOMAG/KOMEKO2021.5.

[5] Biskup T., Cieniuch A, Kołodziej H., Paluszczak D., Sontowski J.: Przekształtnik typu dab w systemie magazynowania energii z akumulatorem niskonapięciowym, Maszyny Elektryczne - Zeszyty Problemowe Nr 1/2022 (127) (in polish).

[6] Hylla P., Trawiński T., Polnik B., Burlikowski W., Prostański D. (2023): Overview of hybrid energy storage systems combined with RES in Poland. Energies, 16(15), 5792. doi:10.3390/en16155792.

[7] Kurpiel W., Polnik B., Miedziński B.: Właściwości eksploatacyjne ogniw litowych. elektro.info 2018, Vol. 10, pp. 44-48.

[8] Kurpiel W.: Research on balancing BMS systems in a climatic chamber. Min. Mach. 2020, 53-63.

[9] Karta katalogowa Ogniwa Winston LFP100AHA WIDE cell. Pobrane z https://files.gwl.eu/inc/_doc/attach/StoItem/3861/ThunderSky-Winston-LIFEPO4-100Ah-WIDE Datasheet.pdf

[10] Karta katalogowa Orion BMS 2 Pobrane z https://www.orionbms.com/products/orion-bms-standard/

[11] https://www.kamitekno.com/itech-it6108c-1500-240-cift-yonlu-programlanabilir-dc-guc-kaynagi-1500v240a108kw (dostęp 07.2024).

[12] Wang C.-Y. (2012): Battery Systems Engineering. New York: John Wiley & Sons Inc.

Publisher: **KOMAG Institute of Mining Technology, Poland**